CHEMIJA
2023. Vol. 34. No. 1. P. 8–18

ISSN 0235-7216 eISSN 2424-4538
DOI: https://doi.org/10.6001/chemija.2023.34.1.2

Multiwavelength Raman spectroelectrochemical study of poly(N-methylaniline): An overview

Regina Mažeikienė,

Gediminas Niaura,

Albertas Malinauskas*

Department of Organic Chemistry,
Center for Physical Sciences and Technology,
3 Saulėtekio Avenue,
10257 Vilnius, Lithuania

Raman spectroscopic study of poly(N-methylaniline) as a thin layer deposited at a electrode was performed in an electrochemical system. A broad range of Raman excitation wavelengths from UV (325 nm) through blue (442 nm) and red (633 nm) to NIR (785 nm) were used. Two limiting redox forms, a reduced (leucoemeraldine) and a fully oxidized one, were considered as obtained at controlled electrochemical potential conditions, and two solution pH of 2.0 and 8.0 were selected to ensure the existence of protonated and deprotonated forms. The Raman spectra obtained and discussed show a strong enhancement for the reduced form at UV and blue laser line excitations, whereas the Raman enhancement for an oxidized form was observed for red and NIR laser line excitations. The main Raman features for the combinations of the reduced and oxidized, and protonated or deprotonated states of poly(N-methylaniline) were analyzed and compared.

Keywords: polyaniline, poly(N-methylaniline), Raman spectroscopy, spectroelectrochemistry, multiwavelength, redox processes

INTRODUCTION

Polyaniline and its derivatives remain attractive materials for potential use in different electrochemical systems. Apart from the parent polymer polyaniline, its chemically modified derivatives possess sometimes specific properties that are of potential interest for various applications. Among them, the polyaniline derivatives chemically substituted at the nitrogen atoms of polymer backbone are of special interest. Substitution of N atoms causes the rearrangement of electronic structure and steric distortions, leading to altered functional properties. N-alkylsubstituted polyanilines present the simplest derivatives of this kind, leaded by the simplest representative poly(N-methylaniline) (PNMA).

* Corresponding author. Email: albertas.malinauskas@ftmc.lt

There have been many reports in the literature on the use of PNMA for specific applications. Many of the recent reports deal with the electrochemistry-related applications of this material. Lithium-sulfur batteries are known to suffer from the dissolution of polysulfides during the charging process, thus, coating the cathode surface by the layer of PNMA was reported to reduce the loss of active material and to improve the cycle stability [1]. A composite of redoped PNMA and multiwalled carbon nanotubes was prepared and used as an active material for creating of a highly selective and sensitive electrochemical sensor for dopamine, that can be used even in the presence of some interfering species [2]. Nanoporous graphitic nitrogen-doped carbon hollow spheres were prepared via the direct pyrolysis of nanostructured PNMA, and enhanced electrochemistry-related properties of the resulting material were reported, including

a high specific capacitance with no loss even after 5,000 cycles of charging-discharging, and an efficient electrochemical oxygen reduction reaction [3]. In order to increase the electric conductivity of PNMA based materials, a special process of synthesis leading to hollow-sphered PNMA nanoparticles with increased conductivity was elaborated [4].

Some works deal with the use of PNMA in corrosion-protective coatings on metal surfaces. Composite PNMA/SiC-ZnO bilayer coatings were prepared onto the carbon steel substrate and evaluated as anticorrosion coatings [5]. Copolymer poly(o-bromophenol-co-N-methylaniline) was prepared electrochemically, and good passivation properties of this copolymer for mild steel in the acid medium were reported [6]. Phosphate-intercalated PNMA composite coatings were prepared at the copper surface in a facile one-step procedure for preventing the copper substrate from corrosion [7]. Other reports deal with the synthesis of chitosan-polyacrylamide gel grafted PNMA for the removal of dye contaminations and bacterial disinfection [8, 9], and PNMA composites with WO_3 for use in perovskite solar cells [10].

For many possible applications of PNMA, fundamental insights into its redox transformations and corresponding changes in its structure are necessary. Raman spectroelectrochemistry presents a very useful tool for the elucidation of electrochemically driven redox and structural changes occuring in this polymer. Previously, we presented a detailed study on the Raman spectroelectrochemistry of polyaniline [11, 12] and PNMA [13] at a broad set of electrode potentials and solution pH values. The present paper has been aimed at an overview of Raman features for two limiting redox forms of PNMA – a reduced and a fully oxidized one – and at the two limiting protonation levels – a protonated and a fully deprotonated one – within a broad Raman excitation range from UV through blue and red to NIR.

EXPERIMENTAL

Much attention has been paid to perform this comparative study under exactly related conditions for each experimental set. We tried to keep the main experimental variables constant throughout an entire work, like the electrode material, electrode configuration and its preparation procedure, the geometry of spectra excitation and the collection of scattered light, as well as the procedure for electrodeposition of a polymer layer. At the same time, changing electrolyte solutions in the electrochemical cell and setting the laser light excitation have been performed in a manner not disturbing an overall experimental layout.

Experimental arrangement for this study was essentially the same as described in details in our previous papers [11, 12, 14]. In short, a cylinder-shaped electrochemical cell has been used in spectroelectrochemical experiments. As a working electrode, a gold electrode of 5 mm in diameter, press-fitted into a Teflon rod holder and placed at about 2 mm distance from the cell optical window, was used. As counter and reference electrodes, a platinum wire and a saturated Ag/AgCl electrode were used, respectively. To reduce possible laser-induced thermo- and photoeffects, and the decomposition of a poly(N-methylaniline) layer by a laser beam, the cell has been periodically moved with respect to the laser beam at a rate of 15–25 mm/s using a custom-built equipment, described in details in Ref. [15]. All electrode potential values given below refer to the saturated Ag/AgCl reference electrode. For each experimental set, the working gold electrode was cleaned with a Piranha solution (a mixture of 30% hydrogen peroxide solution and concentrated sulfuric acid, 1:3 by volume), and then ultrasonicated in a water–ethanol solution for 30 s. Throughout the work, a BASi-Epsilon model (Bioanalytical systems Inc., USA) potentiostat was used.

The layer of poly(N-methylaniline) has been electrodeposited at the working electrode in a separate electrochemical arrangement by applying a controlled potential of 0.8 V for 20 min in a solution containing 0.05 M of N-methylaniline and 0.5 M of sulfuric acid. After that, the electrode was rinsed and placed into a spectroelectrochemical cell. As a working electrolyte, Britton–Robinson buffer solutions of pH 2.0 and 8.0, containing 0.1 M KCl, were used.

Raman spectra were recorded with a confocal microspectrometer inVia (Renishaw, UK) equipped with a thermoelectrically cooled at –70°C CCD camera and a microscope. For the excitation of Raman spectra, the following lasers were used: continuous-wave 325 nm (He-Cd laser, 1 mW, 2400 lines mm^{-1} grating, spectral slit width 9.2 cm^{-1}), 442 nm (He-Cd laser, 4 mW, 2400 lines mm^{-1} grating, spectral slit width 4.5 cm^{-1}), 632.8 nm (He-Ne laser, 1 mW,

1200 lines mm^{-1} grating, spectral slit width 5.4 cm^{-1}) and 785 nm (diode laser, 4 mW, 1200 lines mm^{-1} grating, spectral slit width 4.1 cm^{-1}). The 5x/0.12 NA objective lens was used for the excitation and collection of Raman spectra excited with all visible and NIR laser lines, and a 15x/0.32 NA objective lens was used for the UV laser line excited spectra.

RESULTS AND DISCUSSION

Chemical structures of poly(N-methylaniline)

First, let us consider the chemical structures for different forms of poly(N-methylaniline) in order to discriminate them from those of the parent polyaniline. Figure 1 shows the formal chemical structures for PNMA in its reduced leucoemeraldine base and the salt (*viz*. non-protonated and protonated) forms (PNMA LEB and PNMA LES, respectively, the top two structures in Fig. 1). Oxidation, performed at the stoichiometry of one electron per two aromatic rings, leads to an emeraldine (half-oxidized) form. The 3rd structure from the top in Fig. 1 shows the emeraldine salt form where both electrons are formally withdrawn from the same aromatic ring, thus forming a quinone-like structure. In reality, both cation radicals formed in oxidation are not localized at the same ring, instead, they could be delocalized through the entire polymer

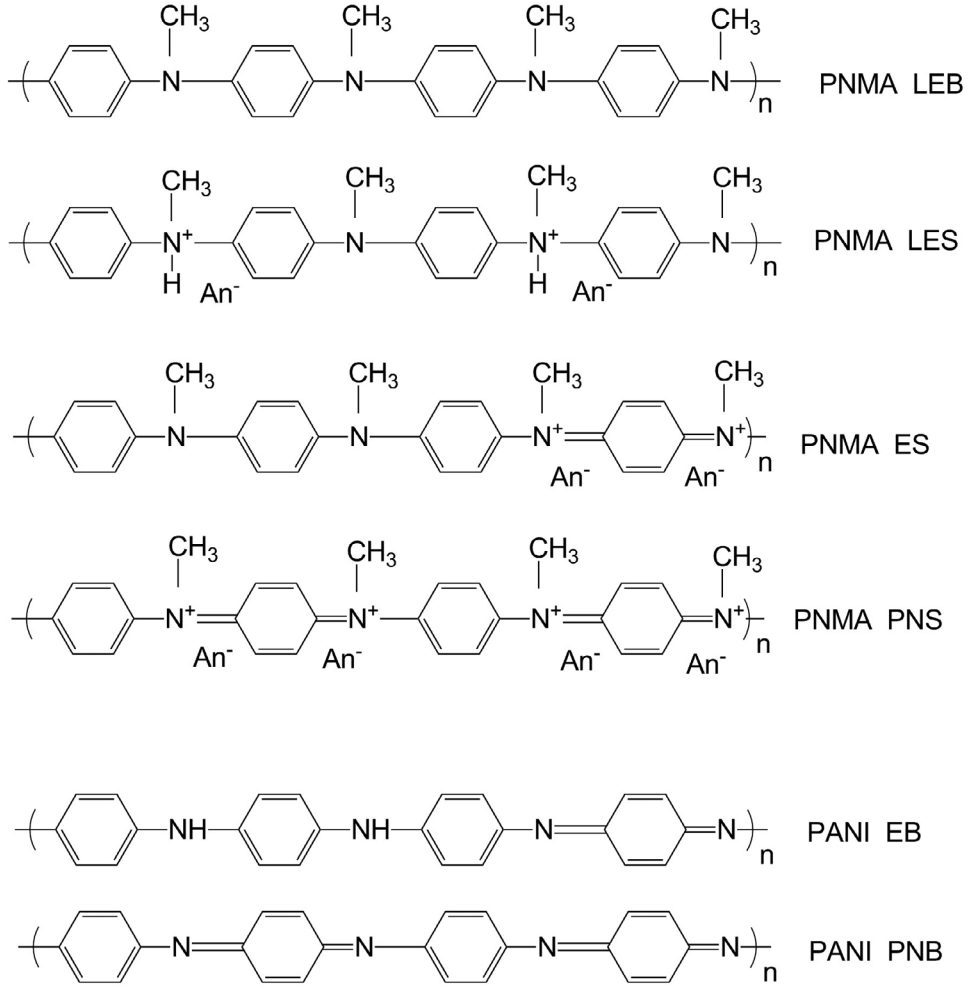

Fig. 1. Chemical structures of four main forms of poly(N-methylaniline) (top four formulas) and two additional polyaniline structures (two bottom formulas), taking into account their different redox and protonation states. Abbreviations: PNMA LEB, poly(N-methylaniline) leucoemeraldine base (fully reduced and deprotonated form); PNMA LES, poly(N-methylaniline) leucoemeraldine salt (fully reduced, protonated and anion-doped form); PNMA ES, poly(N-methylaniline) emeraldine salt (half-oxidized protonated and anion-doped form, shown in its bipolaronic state); PNMA PNS, poly(N-methylaniline) pernigraniline salt (fully oxidized anion-doped form); PANI EB, polyaniline emeraldine base (half-oxidized deprotonated form); PANI PNB, polyaniline pernigraniline base (fully oxidized deprotonated form); An^-, anion

structure. These delocalized cation radicals, or polarons, are responsible for the electric conductance of polymer. As distinct from PNMA, the two half-oxidized forms for polyaniline are possible. In an acidic solution, the protonated form of PANI emeraldine salt appears predominant, whereas the non-protonated PANI emeraldine base prevail in pH-neutral or alkaline solutions, as depicted by the 2nd structure from the bottom in Fig. 1 (PANI EB). It follows from the structural considerations that, unlike PANI, PNMA could not be able to form its emeraldine base form, since this would require the split of C–N bonds, leading again to the PANI structure.

Reduced forms of PNMA

For the study of protonated (salt) and deprotonated (base) forms of PNMA we chose two different solutions with pH values of 2.0 and 8.0, respectively. For these two solutions, electrode potentials of 0.0 and –0.5 V, respectively, were chosen, based on the known data [16, 17], in order to keep the PNMA layer in its fully reduced state. Figure 2 displays the Raman spectra obtained in the pH 2.0 solution at an electrode potential of 0.0 V, corresponding to the fully reduced and protonated form, *viz.* PNMA ES according to Fig. 1. For a detailed analysis of Raman spectra, three main wavenumber ranges should be considered, following our previous work [11]:

i) 1650–1520 cm^{-1} range with the most prominent C–C and C=C bond stretchings, related either to benzene or quinone rings in the polymer backbone, thus indicating an actual redox state of PNMA;

ii) 1520–1210 cm^{-1} range with the most characteristic single, double and intermediate between these two carbo-nitrogen bonds stretchings, again related to the actual redox state of the polymer;

iii) 1210–1050 cm^{-1} range with C–H bond bending vibrations that could be related to the benzene or quinone type rings of polymer backbone.

As it could be expected, the dominating Raman band around 1620 cm^{-1} is observed at the UV (325 nm) and blue (442 nm) laser line excitation,

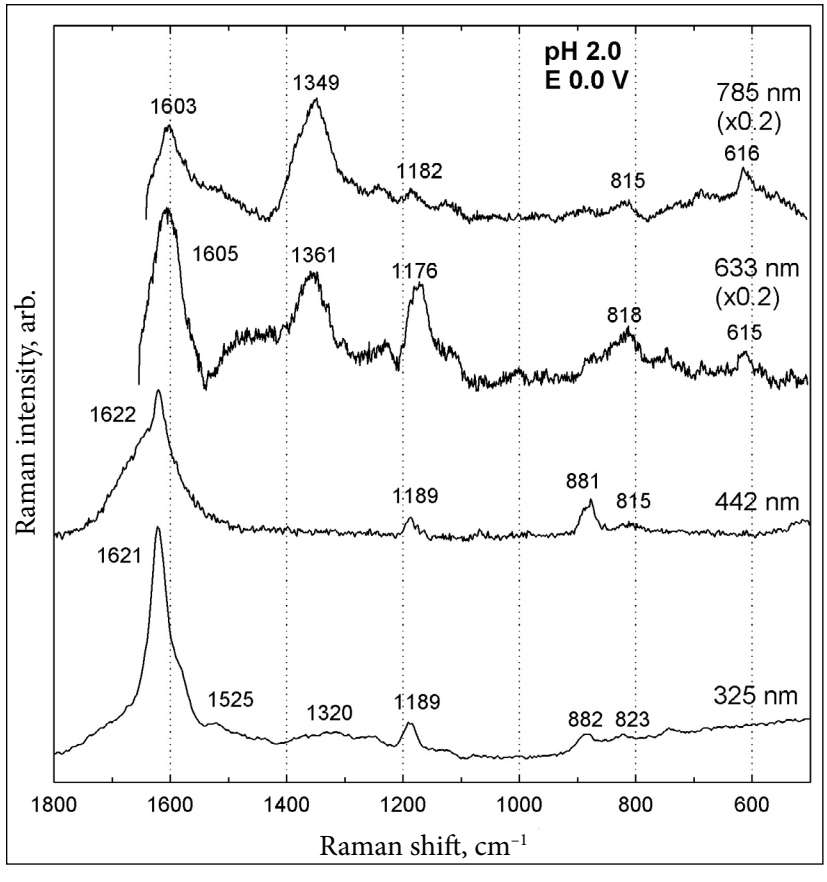

Fig. 2. Raman spectra of the poly(N-methylaniline) layer at a gold electrode, as obtained in the pH 2.0 solution at an electrode potential of 0.0 V (for the reduced and protonated form of PNMA) with different wavelengths of laser line excitation (as indicated)

related to benzene stretching vibrations (Fig. 2). Also, the C–H bond bending vibrations in a leucoemeraldine form of PNMA are well expressed as a mid-intense band at 1189 cm^{-1} for the UV and blue line excitation (Fig. 2). Both these features are characteristic of the reduced leucoemeraldine form. Next to these, few mid- or low-intense Raman bands are observed, related to the benzene ring deformation and C–N–C bending vibrations, as summarized in the Table.

At the red (633 nm) and NIR (785 nm) laser line excitation, intenser and richer in features Raman spectra are observed (Fig. 2). Here again a very strong band related to benzene ring stretchings is observed, somewhat shifted downward as compared to the UV or blue line excitation by 15–20 cm^{-1}. A very strong band around 1360–1350 cm^{-1} is seen at red and especially NIR line excitations (Fig. 2), clearly related to intermediate C~N^+ bond stretching vibrations in a polaronic form of PNMA (Table), thus indicating the presence of polarons within the polymer film. The presence of this band deserves a special consideration. Ideally, a polaronic form should not be present in a reduced leucoemeraldine form. However, we noted previously that for the parent PANI, a strong resonant enhancement of Raman spectra proceeds at the red and especially NIR excitement because both half-oxidized (emeraldine) and fully oxidized (pernigraniline) forms of PANI appear deeply green or blue coloured [18] and thus able to resonance enhancement [11, 12]. Therefore, even the presence of a small amount of half-oxidized and blue coloured emeraldine form within probably a non-ideally electrochemically reduced PANI layer causes a strong enhancement of spectra and the appearance of this feature, characteristic of the presence of polarons [11, 12]. Similarly to the parent PANI, its N-substituted derivatives like PNMA or poly(N-benzylaniline) appear also deeply green or blue coloured in their half- or fully oxidized states [19–22]. Thus, even the presence of a small amount of oxidized species within the electrochemically reduced PNMA film kept at a reducing potential of 0.0 V could lead to the appearance of Raman band, characteristic of a polaronic form. Similarly, we observed polaron-related Raman bands for the reduced form of PANI by turning from the UV or blue to red or NIR spectra excitation under the same electrochemical conditions [14]. In this respect, both PANI and PNMA show a very similar behaviour. However, an interesting difference between PANI and PNMA should be noted. For PANI, switching from the blue to red excitation occurs, next to the appearance of polaron-related bands, also to the appearance of the C=C stretching band characteristic of quinone rings and located around 1590 cm^{-1} [14]. As a result, two ring-related Raman bands, located around 1625 cm^{-1} for benzene type rings and 1590 cm^{-1} for quinone rings, were observed for PANI [14]. For PNMA, however, no separate C=C stretching band appears by switching from the blue to red excitation. Instead, the only Raman band appears, shifted by 15–20 cm^{-1} toward lower wavenumbers (Fig. 2). This single Raman band for PNMA appears almost in the mid position between the two bands for PANI [14]. Therefore, it could be supposed that all C–C bands in the six-member rings of PNMA are equal in terms of their force constants or even bond order, as distinct from distinct single C–C or double C=C bonds in the six-member rings of PANI.

Similarly, the frequencies for C–H bending vibrations also appear shifted by approx. 7–13 cm^{-1} to lower values by switching from the blue to red excitation, although they never reach the corresponding values, characteristic of a half-oxidized emeraldine form (Fig. 2).

Changing the solution pH to 8.0, coupled with the shifting of electrochemical potential to –0.5 V in order to keep the PNMA layer in its reduced and presumably deprotonated form, results in very similar Raman spectra at UV and blue excitation wavelengths (Fig. 3). Some visible differences for the blue excitation relate to a remarkable shift of the C–C stretching band in benzene type rings by approx. 10 cm^{-1} toward higher wavenumbers (Fig. 3). For red and NIR excitations, somewhat more differences are seen. Similarly as for the pH 2.0 solution, intense Raman bands related to the polaronic form of PNMA are observed at 1356–1351 cm^{-1}, showing probably a small amount of oxidized species present within the polymer layer despite of the reduction potential applied. However, as distinct from pH 2.0 solutions, Raman bands related to single C–N bond stretching vibrations around 1241–1231 cm^{-1}, as well as Raman bands related to double C=N bond stretchings at 1472 cm^{-1} (for red excitation), both characteristic of the half-oxidized emeraldine form, are seen (Fig. 3). This means that, in the pH 2.0 solution, the polaronic form

Table. **Characterization of the Raman bands of poly(N-methyl)aniline layer in its reduced and oxidized forms deposited at a gold electrode, as obtained at different spectra excitation laser line wavelengths in pH 2.0 and pH 8.0 solutions**

Solution pH	Raman bands (in cm^{-1}) for different redox forms of poly(N-methyl)aniline and excitation wavelengths								Tentative assignments
	Reduced form				Oxidized form				
	785 nm	633 nm	442 nm	325 nm	785 nm	633 nm	442 nm	325 nm	
2.0	1603(vs)	1605(vs)	1622(vs)	1621(vs)	1625(s)	1630(vs)	1631(vs)	1620(vs)	C–C stretching in B (8a)
8.0	1607(vs)	1612(vs)	1632(vs)	1621(vs)	1621(s)	1633(m)	1633(vs)	1621(vs)	
2.0	–	–	–	–	1596(s)	1591(s)	–	–	C=C stretching in Q (8a)
8.0	–	–	–		1594(s)	1594(s)	–	–	
2.0	–	–	–	1525(w)	1521(m)	1555(w)	–	–	–
8.0	–	–	–	1524(w)	1518(w)	1554(w)	–	–	
2.0	–	–	–	–	–	1483(vs)	–	–	C=N stretching in emeraldine base (imine sites)
8.0	1443(w)	1472(s)	–	–	–	1477(vs)	–	–	
2.0	–	–	–	–	–	1441(w)	1438(w)	1448(vw)	–
8.0	–	–	–	–	–	–	1413(w)	1444(w)	
2.0	–	–	–	–	1391(m)	1377–57	–	–	C~N^+ stretching in polaronic form (polarons)
8.0	–	–	–	–	1390(m)	1371–52			
2.0	1349(vs)	1361(vs)	1320(w)	–	1353(s)	1325(w)	–	–	
8.0	1351(vs)	1356(s)	1320(w)	–	1345(vs)	1321(w)	–	–	
2.0	1241(w)	1231(w)	–	–	1230(w)	1225(m)	–	–	C–N stretching in emeraldine (amine sites)
8.0	1231(m)	1230(vw)	–	–	1222(w)	1220(m)	–	–	
2.0	1182(m)	1176(s)	1189(m)	1189(m)	1185(vs)	1185(sh)	–	–	C–H bending in leucoemeraldine (9a)
8.0	1181(w)	–	1186(m)	1182(m)	–	–	–	1185(w)	
2.0	–	–	–	–	–	1164(vs)	–	–	C–H bending in emeraldine (9a)
8.0	1164(m)	1165(m)	–	–	1163(vs)	1167(vs)	–	–	
2.0	–	–	–	–	1127(m)	–	–	–	
8.0	–	–	–	–	1130(sh)	–	–	–	
2.0	–	–	–	–	976(m)	967(w)	–	–	
8.0	–	–	–	–	971(m)	–	987(w)	–	
2.0	–	–	881(m)	882(w)	861(w)	850(w)	880(m)	888(m)	B deformation (1)
8.0	–	–	874(w)	–	860(sh)	–	873(w)	–	
2.0	815(m)	818(m)	815(vw)	823(w)	806(s)	811(m)	–	–	C–N–C bending
8.0	819(m)	811(w)	–	–	805(m)	–	–	–	
2.0	–	–	–	–	–	795(s)	–	–	Q deformation
8.0	–	–	–	–	–	786(m)	–	–	
2.0	–	747(w)	–	745(w)	745(m)	755(m)	–	–	Imine deformation (C–N–C bending)
8.0	744(w)	747(vw)	–	–	745(m)	749(w)	–	–	
2.0	616(m)	615(m)	–	–	–	–	–	–	Ring deformation (6b)
8.0	617(m)	617(w)	–	–	618(w)	616(w)	–	–	
2.0	–	–	–	–	587(w)	585(w)	–	–	Ring deformation (6b)
8.0	–	–	–	–	–	–	–	–	
2.0	–	–	–	–	535(m)	535(m)	531(vw)	–	Amine in-plane deformation
8.0	–	–	–	–	535(m)	529(w)	533(vw)	–	

Assignments are based mainly on the known data [11–14, 24–28]. The numbers given in parentheses (1), (6b), (8a) and (9a) refer to the Wilson's notation of aromatic species vibration modes. Abbreviations used: B: benzene type ring, Q: quinone type ring, (vs): very strong, (s): strong, (m): mid-intense, (w): weak, (vw): very weak, (sh): shoulder, ~: bond intermediate between a single and a double, –: the band of very weak or even undetectable intensity. Spectra for the reduced form of polyaniline were obtained at a controlled electrode potential of 0.0 V for pH 2.0 solution, or –0.5 V for pH 8.0 solution, and the spectra for the oxidized form were obtained at a controlled potential of 0.8 V for pH 2.0 solution, or 0.3 V for pH 8.0 solution.

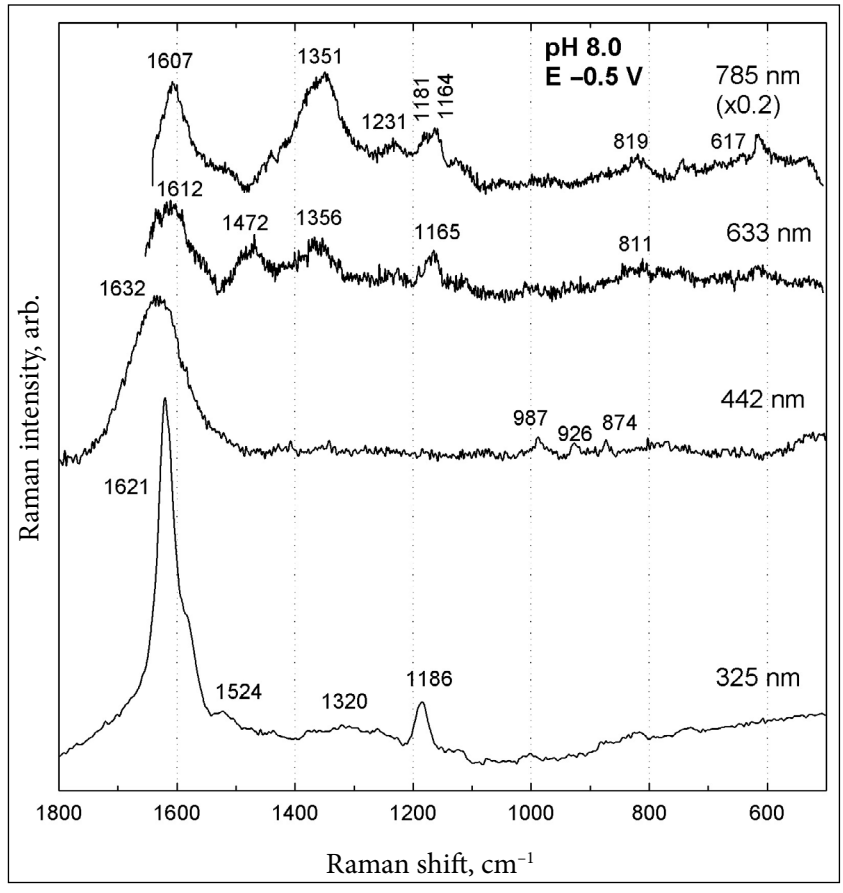

Fig. 3. Same as in Fig. 2, as obtained in the pH 8.0 solution at an electrode potential of –0.5 V (for the reduced and deprotonated form of PNMA)

prevails among this small amount of oxidized species present within the polymer layer, whereas an equilibrium between polaronic and other oxidized forms containing double C=C bonds exists within the polymer film at pH 8.0. Also, as distinct from the pH 2.0 solution, the C–H bending vibrations of an emeraldine form, located around 1165 cm^{-1}, next to the C–H bendings of a reduced leucoemeraldine form, located around 1180 cm^{-1}, are seen for the red and especially NIR excitation (Fig. 3). The assignments of the Raman bands observed are presented in the Table.

Oxidized forms of PNMA

For the study of the oxidized forms of PNMA, again, the same solutions with pH 2.0 and 8.0 were chosen, whereas the electrochemical potential has been shifted by 0.8 V toward the positive direction in order to ensure a full oxidation of the polymer layer, *viz.* up to 0.8 V for pH 2.0 and 0.3 V for pH 8.0. The structures for the oxidized forms of PNMA are presented in Fig. 1. Because of the presence of methyl groups at nitrogen atoms, only two 'classic' forms for PNMA are possible: a half-oxidized emeraldine salt form (PNMA ES) and a fully oxidized pernigraniline salt form (PNMA PNS). As distinct from PANI, no non-protonated oxidized forms for PNMA are expected, since these would require the demethylation of the polymer backbone leading to PANI-like structures. Also, as distinct from PANI, both oxidized forms of PNMA bear positive charges, and thus they require their doping by negative anions (Fig. 1).

Figure 4 shows the Raman spectra for the oxidized form of PNMA as obtained in the pH 2.0 acidic solution at a relatively high electrochemical potential of 0.8 V. At UV and blue laser line excitations, the spectra appear poor in their properties. The most intense bands located at 1620 and 1631 cm^{-1} for UV and blue excitations, respectively, appear dominating over the entire spectrum and obviously belong to the C–C stretchings in benzene rings. Most important, no Raman bands are observed around 1595–1590 cm^{-1}. Although the polymer presents in its oxidized form under the experimental conditions specified for

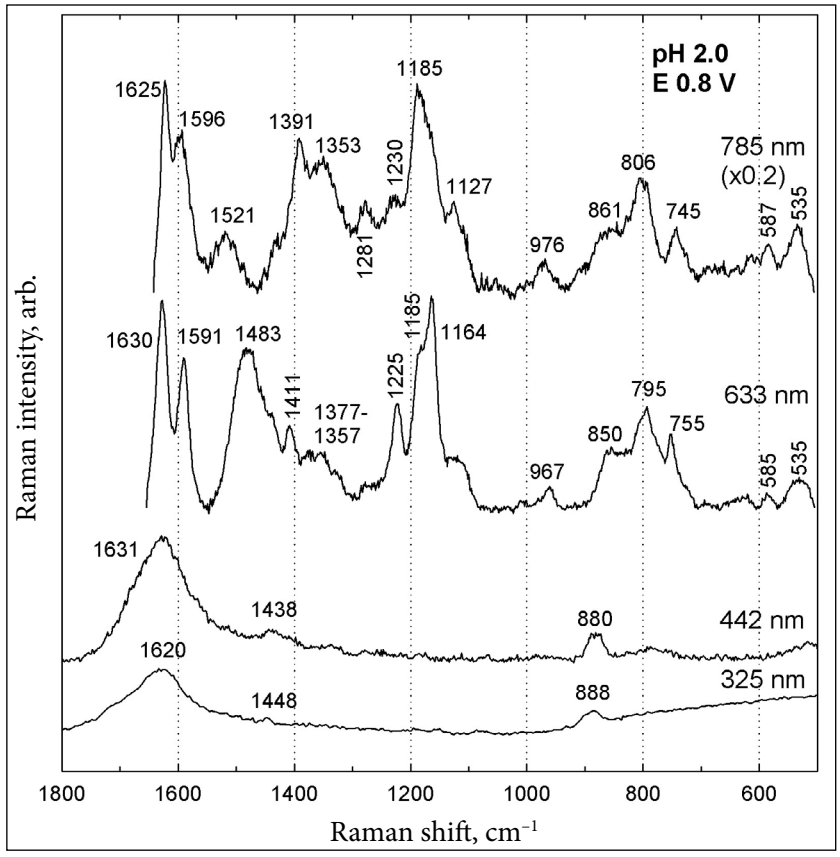

Fig. 4. Same as in Fig. 2, as obtained in the pH 2.0 solution at an electrode potential of 0.8 V (for the oxidized and protonated form of PNMA)

Fig. 4, there are no signs for this, i.e. for the presence of quinoid-like rings, specific of oxidized species. The most probable reason for this is that the wavelengths used in the excitation of spectra, 325 and 442 nm, are in resonance with the reduced species, thus leaving the oxidized forms 'invisible'. This effect has been discussed previously for PANI, as observed at the same excitation wavelengths [11, 12, 14].

Rich in features Raman spectra are obtained for red and NIR laser line excitations (Fig. 4). The entire intensity of Raman spectra also appears higher at these excitation wavelengths, especially for the 785 nm line. Here, next to the presence of usual very intense Raman features for the C–C stretchings in benzene rings, located at 1630 and 1625 cm^{-1} for 633 and 785 nm line excitations, respectively, intense bands located around 1591 and 1596 cm^{-1} for the two said excitation wavelengths are also present, characteristic of the C=C stretching vibrations in quinone type rings, thus indicating the presence of oxidized species. For the 633 nm excitation, a very intense band located around 1483 cm^{-1}, characteristic of the C=N stretchings in emeraldine (i.e. for imine sites), also reveals the oxidized state of PNMA under specified conditions. Interestingly, no well-expressed band for the C=N stretchings is observed for the 785 nm excitation (Fig. 4). The probable reason for this could be as follows. For the oxidized PNMA, two principal species are possible. One of them relates to the structures containing two cation radicals localized at the same aromatic ring, as depicted in the structure denoted as PNMA ES in Fig. 1 (the bipolaronic structure). In reality, however, the cation radicals could be delocalized and not related to the same aromatic ring (polaron structure). Both these structures are very probably present in a dynamic equilibrium. Since the polymer layer used in obtaining of Raman spectra at 633 and 785 nm excitations, as presented in Fig. 4, is exactly the same considering its redox and protonation state, the differences observed in its spectra for different excitation wavelengths are most probably related to somewhat different resonance conditions. It is very probably that, at the 633 nm excitation, the resonance refers mostly to a bipo-

laronic form. Indeed, an intense band at 1483 cm^{-1} for the 633 nm excitation, as well as its absence for the 785 nm excitation indicate very probably a resonance of 633 nm excitation with the bipolaronic form. Similarly, the Raman band located around 1225 cm^{-1} for the 633 nm excitation, indicative of the C–N stretchings in emeraldine, appears more intense than the corresponding band located at 1230 cm^{-1} for the 785 nm excitation, also indicating that bipolaronic form-related features are resonantly enhanced at the 633 nm excitation. At the same time, the Raman bands within the approximate range of 1400–1350 cm^{-1} are well known to be indicative of the presence of delocalized polarons. Previously, we have discussed these Raman features in details [23]. It is seen from Fig. 4 that both red and NIR excitations yield a few bands within this range, related to polarons. However, the intensity for these bands appears much higher for the 785 nm excitation as compared to the 633 nm one. This indicates that, owing to exactly the same redox state of PNMA layer at both these excitation wavelengths, the polaron-related features appear better expressed at the 785 nm excitation, although both these excitation wavelengths favour the appearance of polaron features, as distinct from UV and blue laser line excitations. In summary, it could be concluded that the 633 nm excitation of Raman spectra favours the enhancement of bipolaron-related features, whereas the 785 nm excitation tends to reveal polaron-related features. Other Raman features, obtained for the oxidized PNMA layer at different excitation wavelengths, are summarized in the Table.

Turning now to the alkaline solution of pH 8.0, it should be noted that the cores of spectra for the oxidized form of PNMA appear quite similar to those observed at pH 2.0 (Fig. 5). This appears to be not unexpected, since there should be no 'deprotonated' form of oxidized PNMA, as distinct from the parent PANI, as it follows from the consideration of their chemical structures presented in Fig. 1. At UV and blue line excitations, again, the C–C stretchings in benzene rings appear dominant over the entire spectra, located at 1621

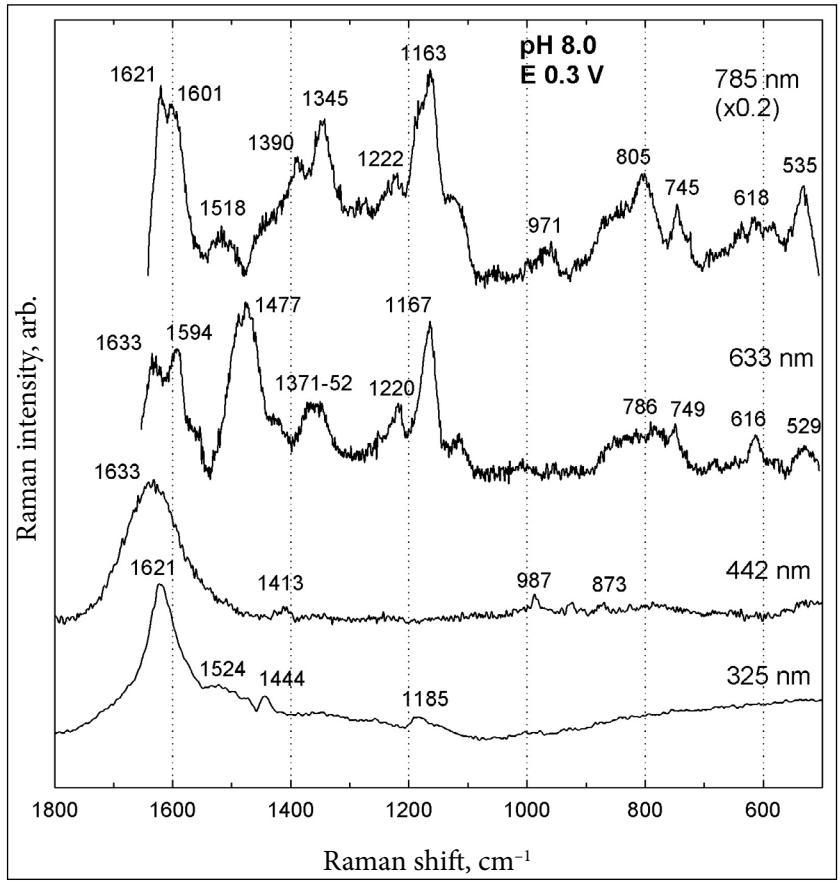

Fig. 5. Same as in Fig. 2, obtained in the pH 8.0 solution at an electrode potential of 0.3 V (for the oxidized and deprotonated form of PNMA)

and 1633 cm^{-1} for 325 and 442 nm excitations, respectively (Fig. 5). Again, no visible signs for the C=C stretching vibrations in quinone type rings are observed. At the red and NIR laser line excitations, however, both these features are well observed, indicating that a layer of PNMA presents in its oxidized form (Fig. 5). As for the interplay of C=N stretchings and polaron-like stretchings, it follows the same way as for the acidic solution. At the 633 nm excitation, C=N stretchings are observed as a very intense band around 1477 cm^{-1}, whereas characteristic polaron bands appear as a mid-intense couple of bands within the range of 1371–1352 cm^{-1} (Table). At the 785 nm excitation, however, mid- to very intense bands at 1390 and 1345 cm^{-1} are observed (Fig. 5), following the same way as for the pH 2.0 solution (cf. with Fig. 4). All Raman bands observed are summarized in the Table.

CONCLUSIONS

The four excitation wavelengths applied reveal different Raman features for the same redox state of PNMA. At UV (325 nm) and blue (442 nm) excitations, the electrochemically reduced leucoemeraldine form of PNMA appears to be in a spectral resonance, both in acidic (pH 2.0) and alkaline (pH 8.0) solutions, showing the C–C stretching vibrations within a range of 1632–1603 cm^{-1} as a dominant feature. Far more intense Raman spectra for the same reduced form are observed at red (633 nm) and NIR (785 nm) excitations. Next to the C–C stretchings, intense polaron-related Raman bands around 1350 cm^{-1} appear at these excitation wavelengths.

For the electrochemically oxidized form of PNMA, again, C–C stretching vibrations are dominating over the entire spectrum at the UV and blue laser line excitations both in acidic and alkaline solutions, showing no signs for oxidized species, very probably due to the resonance with the reduced form. For the red and NIR line excitations, however, specific features for oxidized species are well seen like, e.g. the C=C stretching vibrations in quinone type rings located in a range of 1601–1591 cm^{-1}. A high intensity of the spectra for these two excitations observed also shows a resonance with the oxidized form of PNMA. At the 633 nm excitation, C=N stretchings appear very intense indicating the oxidized form to be prevalent both in acidic and alkaline solutions. Polaron-related Raman bands, located within a range of 1391–1345 cm^{-1}, appear well developed especially at the NIR excitation. In general, the red laser line excitation at 633 nm favours the observation of C=N stretchings, whereas the NIR line excitation reveals especially polaron-like stretching vibrations.

Received 16 January 2023
Accepted 31 January 2023

References

1. C. Y. Shi, B. Hong, X. Y. Zhang, et al., *J. Electroanal. Chem*., **871**, Art. No. 114312 (2020).
2. C. Direksilp, J. M. Scheiger, N. Ariyasajjamongkol, A. Sirivat, *Anal. Methods*, **14**, 469–479 (2022).
3. P. Bairi, K. Sardar, M. Samanta, K. Chanda, K. K. Chattopadhyay, *Mater. Chem. Frontiers*, **5**, 7645–7653 (2021).
4. C. Direksilp, A. Sirivat, Polymers, **12**, Art. No. 1023 (2020).
5. C. B. Hu, Y. Li, T. Z. Li, et al., *Coll. Surf. A Physicochem. Engn. Aspects*, **585**, Art. No. 124176 (2020).
6. G. M. Abd El-Hafeez, M. M. El-Rabeie, A. F. Gaber, Z. R. Farag, *J. Coat. Technol. Res*., **18**, 581–590 (2021).
7. H. Liu, B. M. Fan, G. F. Fan, et al., *J. Alloys Compounds*, **872**, Art. No. 159752 (2021).
8. H. G. Mohamed, A. A. Aboud, H. M. Abd El-Salam, *Intern. J. Biol. Macromol*., **187**, 240–250 (2021).
9. M. S. Alshammari, A. A. Essawy, A. M. El-Nggar, S. M. Sayyah, *J. Chem*., **2020**, Art. No. 3297184 (2020). DOI: 10.1155/2020/3297184.
10. M. O. Yildirim, E. C. Gok, N. H. Hemasiri, et al., *Chempluschem*, **86**, 785–793 (2021).
11. R. Mažeikienė, G. Niaura, A. Malinauskas, *Synth. Metals*, **243**, 97–106 (2018).
12. R. Mažeikienė, G. Niaura, A. Malinauskas, *Synth. Metals*, **248**, 35–44 (2019).
13. R. Mažeikienė, G. Niaura, A. Malinauskas, *Spectrochim. Acta Part A Mol. Biomol. Spectrosc*., **274**, (2022) Art. No. 121109.
14. R. Mažeikienė, G. Niaura, A. Malinauskas, *J. Solid State Electrochem*., **23**, 1631–1640 (2019).
15. G. Niaura, A. K. Gaigalas, V. L. Vilker, *J. Raman Spectrosc*., **28**, 1009–1011,(1997).
16. R. Sivakumar, R. Saraswathi, *Synth. Metals*, **138**, 381–390 (2003).
17. K. Brazdžiuvienė, I. Jurevičiūtė, A. Malinauskas, *Electrochim. Acta*, **53**, 785–791 (2007).
18. A. Malinauskas, R. Holze, *Synth. Metals*, **97**, 31–36 (1998).

19. N. Comisso, S. Daolio, G. Mengoli, R. Salmaso, S. Zecchin, G. Zotti, *J. Electroanal. Chem*., **255**, 97–110 (1988).
20. M. V. Kulkarni, A. K. Viswanath, P. K. Khanna, *Sens. Actuat. B Chem*., **115**, 140–149 (2006).
21. M. V. Kulkarni, A. K. Viswanath, P. K. Khanna, *J. Appl. Polym. Sci*., **99**, 812–820 (2006).
22. A. Malinauskas, R. Holze, *J. Solid State Electrochem*., **3**, 429–436 (1999).
23. G. Niaura, R. Mažeikienė, A. Malinauskas, *Synth. Metals*, **145**, 105–112 (2004).
24. M. Lapkowski, K. Berrada, S. Quillard, G. Louarn, S. Lefrant, A. Pron, *Macromolecules*, **28**, 1233–1238 (1995).
25. S. Quillard, K. Berrada, G. Louarn, S. Lefrant, M. Lapkowski, A. Pron, *New J. Chem*., **19**, 365–374 (1995).
26. M. Lapkowski, K. Berrada, S. Quillard, G. Louarn, S. Lefrant, *J. Chim. Phys. Phys. Chim. Biol*., **92**, 915–918 (1995).
27. M. Boyer, S. Quillard, G. Louarn, S. Lefrant, E. Rebourt, A. P. Monkman, *Synth. Metals*, **84**, 787–788 (1997).
28. M. C. Bernard, A. Hugot-Le Goff, *Synth. Metals*, **85**, 1145–1146 (1997).

Regina Mažeikienė, Gediminas Niaura, Albertas Malinauskas

DAUGIABANGIS RAMANO SPEKTROELEKTROCHEMINIS POLI(N-METILANILINO) TYRIMAS: APŽVALGA

S a n t r a u k a

Atliktas Ramano spektroskopinis poli(N-metilanilino) plono sluoksnio, nusodinto ant elektrodo paviršiaus, tyrimas. Ramano spektrai buvo sužadinami kelių skirtingų bangos ilgių šviesa: ultravioletine (325 nm), mėlyna (442 nm), raudona (633 nm) ir artimųjų infraraudonųjų (785 nm). Tyrimams naudotos dvi kraštinės polimero redokso formos – redukuota (leukoemeraldino) ir visiškai oksiduota, kurios buvo gaunamos palaikant tinkamą elektrocheminį potencialą. Abi formos tirtos pH 2,0 ir 8,0 tirpaluose, taip užtikrinant jų protonuotą ir deprotonuotą būsenas. Gauti rezultatai atskleidė rezonansinį redukuotos polimero formos spektrų stiprinimą, naudojant ultravioletinį ir mėlynąjį sužadinimą bei rezonansinį oksiduotos formos spektrų stiprinimą, naudojant raudonąjį bei artimąjį infraraudonąjį sužadinimą. Nuodugniai aptariami abiejų redokso formų spektrų ir struktūrų ypatumai.